

Ultra-narrow bandpass optical interference filters for deep space optical communication.

Thomas Rahmlow, Timothy Upton, Markus Fredell, Terry Finnell, Stephen Washkevich,
Kirk Winchester, Tina Hoppock and Robert Johnson
Omega Optical, Inc.
Brattleboro, Vermont

Proc. SPIE 10524, Free-Space Laser Communication and Atmospheric Propagation XXX, 1052416 (2018);
doi:10.1117/12.2290753

Copyright 2019 Society of Photo-Optical Instrumentation Engineers. One print or electronic copy may be made for personal use only. Systematic reproduction and distribution, duplication of any material in this paper for a fee or for commercial purposes, or modification of the content of the paper are prohibited.

Ultra-narrow bandpass optical interference filters for deep space optical communication.

Thomas Rahmlow, Timothy Upton, Markus Fredell, Terry Finnell, Stephen Washkevich, Kirk Winchester, Tina Hoppock and Robert Johnson

**Omega Optical, Inc.
Brattleboro, Vermont**

Abstract

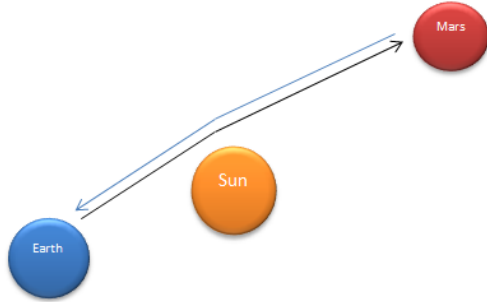
Deep space optical communication is a highly efficient alternative to radio frequency (RF) technology offering higher data bandwidths. The challenge is that deep space optical communication is photon limited. Rejection of extraneous light is critical to maximizing signal quality. High transmitting, ultra-narrow bandpass filters with high out of band optical density (OD) can meet this requirement while improving signal throughput. Design trade-offs and fabrication results are presented for ultra-narrow bandpass filters with bandwidths as narrow as 0.2 nm full width half maximum (FWHM) with on-band transmission greater than 95% and off band rejection of greater than OD 5. Filters are designed to match laser wavelengths in the region of 1550 nm.

1.0 Introduction

Optical communication offers the potential of increasing data bandwidth by as much as 40 times while significantly reducing the weight and power consumption of the flight terminal station compared to radio frequency technology¹. A key requirement of a deep space optical communication link is the need for high rejection of stray and ambient light with high on-band transmission. Ultra-narrow bandpass interference filters with a bandwidth of less than 0.2 nm provide this capability. A challenge of manufacturing ultra-narrow band pass filters is the need to precisely tune the filter's passband wavelength across the full aperture of the filter. The approach to achieving high uniformity presented here is laser targeted annealing.

Optical filters are needed to maximize signal to noise between an earth based station and a satellite or probe located in deep space. The target mission is optical communication between an earth station and Mars orbiter and probe. The optical interference filters must pass the faint laser light while rejecting ambient sunlight and background star light. The most challenging requirement for the filters is to maintain adequate signal-to-noise when the earth and Mars are in opposition and the communication path is within 5° of the sun². Figure 1 presents a schematic of the mission challenge.

- Deep Space Optical Communication has the potential for higher data rates and information density.
- Once developed, the protocol can handle a large number of channels in parallel.



Ground Terminal:

- 1550.1 nm, 0.175 nm FWHM 'Flat Top' ultra-narrow bandpass filter
- 3° operating angle
- Thermally tunable
- Well collimated (F#48) beam
- > OD 12 off-band rejection

Flight Terminal:

- 1064 nm FWHM 'Flat Top' bandpass filter
- Space qualified, thermally stable

- Signal strength is very low: photon counting
- Very high background noise: can be within 5% of the sun when Earth and Mars are in opposition.

Figure 1: This schematic presents the challenges of optical communication over large distances and emphasizes the need for high off band rejection of ambient and stray light.

2.0 Filter Design

The basic design of an optical interference bandpass filter is a Fabry Perot³. This design consists of a pair of mirrors separated by an optical cavity. The optical thickness of the optical cavity layer places the reflection of each mirror out of coherence with each other and thus determines the center passband wavelength. The design is relatively insensitive to thickness errors in the thin films making up the reflector stacks but is very sensitive to errors in the cavity layer and those layers adjacent to the cavity layer. For a single cavity Fabry Perot filter, errors in the cavity layer move the center passband wavelength but do not significantly degrade the shape or peak transmission of the passband.

Figures 2 and 3 illustrate these sensitivities. Figure 2 presents the modeled transmission for a single cavity passband design using a Monte Carlo simulation of random layer thickness errors. Figure 3 presents a plot of the relative sensitivity of each layer on performance. The impact of layer thickness error is modeled by making a small error in layer thickness and comparing the change in the filter's merit function with similar changes in the other layers in the design. The most sensitive layer is the cavity layer.

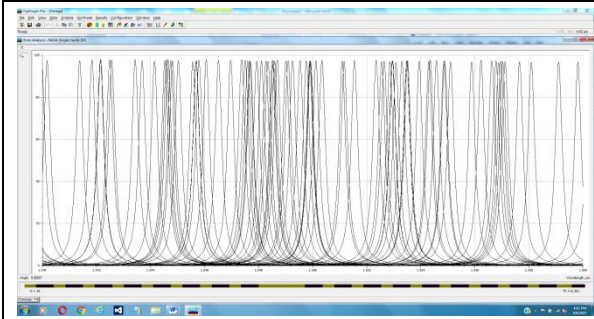


Figure 2: Transmission for 100 trials of a Monte Carlo simulation of a 0.5 nm single cavity design assuming a 1% error in layer thickness is overlaid. Random errors in layer thickness for a single cavity Fabry-Perot design do not tend to distort the shape or band width, only the center wavelength.

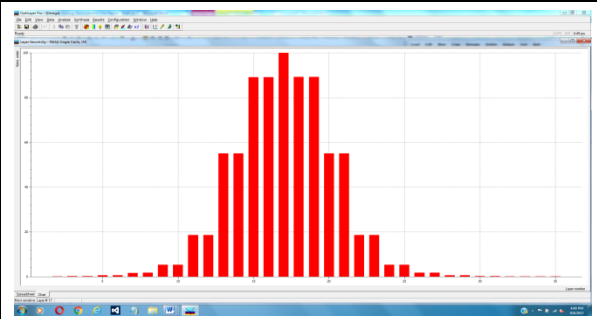


Figure 3: Relative sensitivity of thickness layer errors by layer. The impact of error is greatest for errors in the thickness of the central cavity layer. Single cavity designs can be manufactured with good yield provided the resulting filters can be either angle tuned or annealed to wavelength.

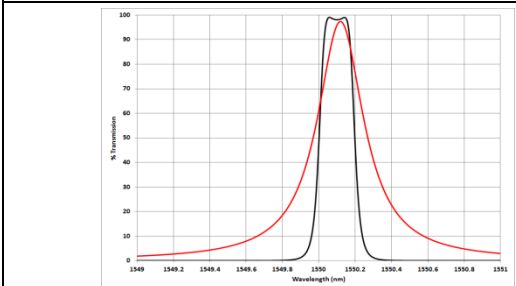


Figure 4: The transmission of a single cavity (red) and multi-cavity (black) bandpass filter designed to the same bandwidth is overlaid. The multi-cavity design gives a flat top response and a sharper edge and deeper skirt.

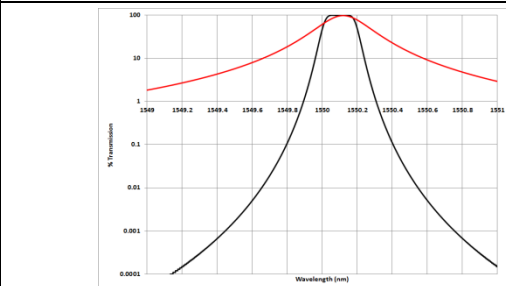


Figure 5: The filter designs presented in figure 4 are plotted on a log scale. The multi-cavity design drives down to an OD of 6 within 1 nm of the CW. Signal to noise for the multi-cavity is 7.4x better than the single cavity.

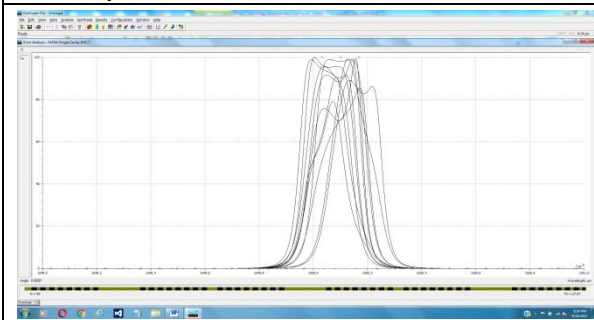


Figure 6: Transmission for 10 trials of a Monte Carlo simulation of a 0.175 multi-cavity design for a 0.005% error in layer thickness is overlaid. Random errors in layer thickness for the multi-cavity design distort the bandpass shape and suppress in band transmission.

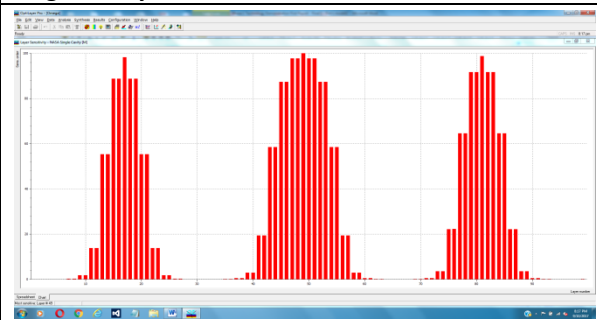


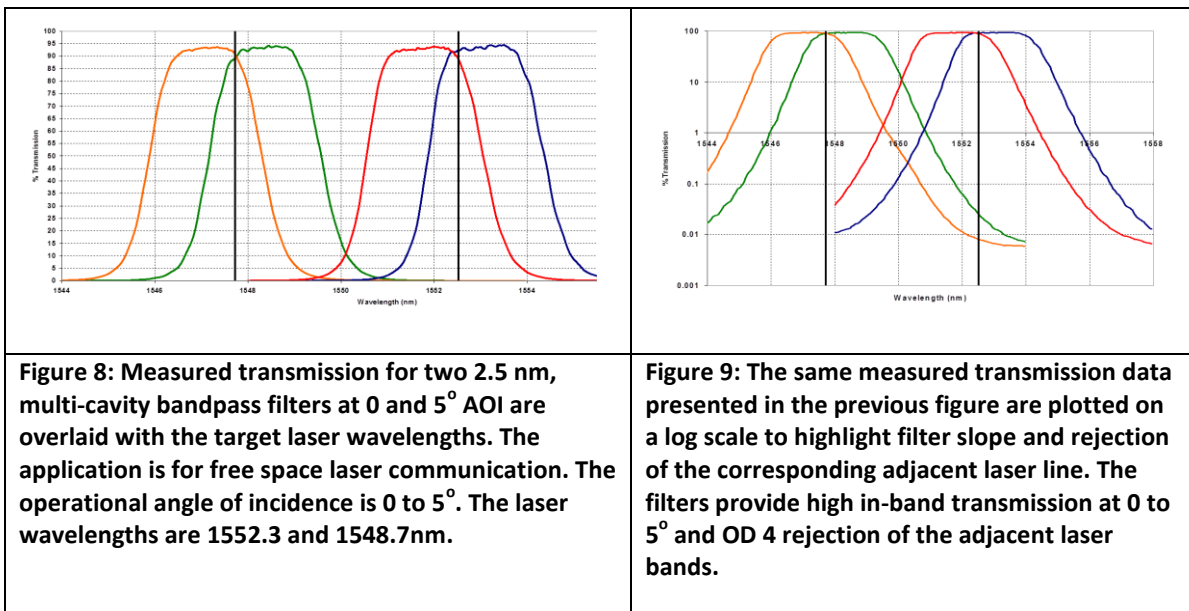
Figure 7: Relative sensitivity of thickness layer errors by layer. The design is comprised of three cavities. Thickness errors in any of the three cavity layers drives the filter out of coherence and destroys the filter's in band transmission.

The Monte-Carlo simulation randomizes the errors applied to each layer. The simulation shows the modeled performance to shift in central wavelength on the whole to be relatively similar in filter bandwidth, peak transmission, and shape. The result is a filter with an error in the central wavelength but in all other respects a very usable filter. In many cases, depending on the choice

of filter materials, the center wavelength can be either angle-tuned to the design wavelength or post-processed using annealing techniques to tune the filter to the design wavelength.

The limitation of the single cavity filter is that it has a characteristically pointed (or triangle shaped) transmission band. A much preferred design is the “flat top” performance that can be realized from using a multi-cavity design. Figure 4 presents an overlay of a single cavity and multi-cavity bandpass filter. Figure 5 presents both designs with transmission plotted on a log scale. The flat top design offers better on-band transmission across the laser’s stability range, steeper edge slope, and deeper optical density “skirts.” The ratio of the sum of in-band transmission to out-of-band transmission for the single cavity is 0.563 and 4.14 for the multi-cavity. This suggests that the signal to noise is 7.4x better for the multi-cavity than for the single cavity design.

The manufacturing challenge of making a multi-cavity design is the need to match each of the cavities to the same central wavelength. Figure 6 presents a set of 10 transmission plots generated using a Monte-Carlo simulation with a thickness error of only 0.005%. Thickness errors distort the band shape, transmission and location of the pass band. Figure 7 presents a layer sensitivity simulation and highlights the sensitivity of the cavity layers.



The manufacture of commercial “flat-top” multi-cavity bandpass filters with a bandwidth of 1 nm and greater at 1550 nm is well demonstrated and within the capabilities of high precision, commercial optical coating equipment and metrology. Figures 8 and 9 presents an example of such a filter set manufactured for free space laser communication between a ground terminal and an aerial target⁴. The fabrication of a sub-nanometer single cavity bandpass filter is also within the capability of current equipment as illustrated for the measured transmission of three single cavity filters⁵ presented in Figure 10. However, manufacturing a sub-nanometer bandpass (0.175 nm) filter pushes the limitations in uniformity and thickness control of the current state of the art process equipment.

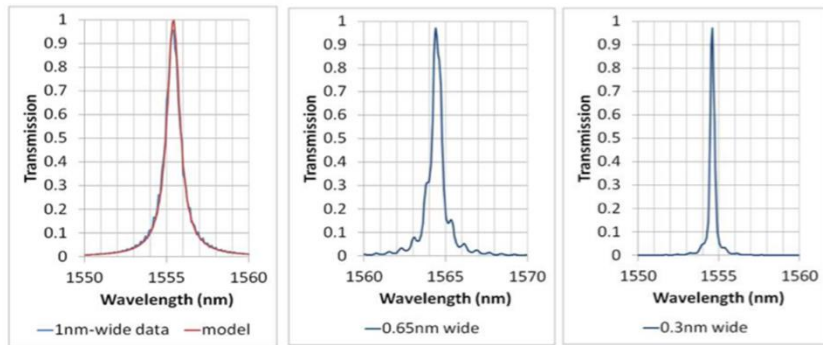


Figure 10: Measured transmission of three ultra-narrow notch filters is presented. These are laser wavelength scanning data for 1.0nm wide, 0.65nm wide, and 0.3nm wide bandpass filters. Ultra-narrow notch bandpass filters can be reliably fabricated, but spectral shift with angle and temperature need to be matched to system requirements. (SPIE Paper 9612-21: Sub-nanometer band pass coatings for LIDAR and astronomy)

3.0 Approach

Test filters were fabricated using a Helios class dual magnetron, plasma assisted deposition system which uses a state of the art optical monitor system for layer termination (Figures 12 and 13). This machine reliably meets uniformity across a 200 mm plate of +/-0.25% of the center wavelength. At 1550 nm, 0.25% non-uniformity translates to a gradient error of 0.75 nm across a 25.4 mm aperture. This non-uniformity is 100x too high to produce high quality 0.175 nm target bandwidth filters. A photograph of the Helios sputtering chamber and cleanroom is presented in figure 11.

The approach we have developed to improve uniformity and tune the filter to a specific wavelength is a post deposition annealing technique for locally target annealing the filter. Post deposition annealing for wavelength tuning of narrow bandpass filters has been used for some time with typical permanent wavelength adjustment of up to 15 nm for single cavity designs and 6 to 8 nm for multi-cavity filter designs without loss of shape.

The center wavelength of the ultra-narrow bandpass filters are monitored in real time using a wavelength scanning laser ⁶. Figure 12 presents a photograph of the laser spectrometer used for these tests. In this photograph, the filter is placed in a donut heater. The heater can achieve up to 500 C in the center core. The position of the center wavelength is monitored as the part is thermally annealed. The apparatus is mounted on an X-Y stage and transmission across the part can be measured.

Initial experiments were made using the thermal heater. The heater does not allow of targeting specific regions on the substrate. In order to achieve localized heating, laser targeted annealing

was used to achieve precision tuning for surface uniformity. A CO₂ laser was used to locally heat regions of the filter and shift performance to the required center wavelength.

Figure 13 presents the measured wavelength shift as a function of power setting. This figure shows the expected “elastic” or thermal expansion region at low delivered energy levels followed by a nominally linear “inelastic” or annealing region as the delivered energy is increased. From this data a look-up table can be generated to determine the settings required to affect a given wavelength shift.



Figure 11: The Helios multi-target high volume reactive sputtering coater provides high volume capability and reliable performance for the most challenging designs.

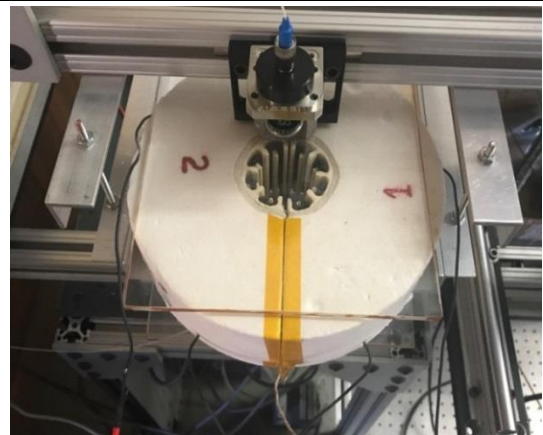


Figure 12: The ultra-narrow band filters are measured using a fiber coupled scanning laser. In this photograph, the filter is placed in a high temperature heater and monitored as it is annealed.

4.0 Annealing Results

Once the response to laser annealing is determined, the uniformity of the filter can be improved using selective (or targeted) annealing. Figure 14 shows the spatial distribution of the center wavelength over a 200mm diameter 1554.0nm filter plate. This measurement displays the 1% variation in the CWL typical of a high performance production coating run. At 1550nm, the wavelength across the plate varies by roughly 15nm. Figures 15 and 16 present results after laser targeted annealing. The center 110 x 110 mm region was laser targeted annealed. The data shows that the center area has been annealed uniform to +/-0.05%. The average center wavelength over this area was measured to be 1554.61 nm. The target wavelength for this test run was 1554.6 nm.

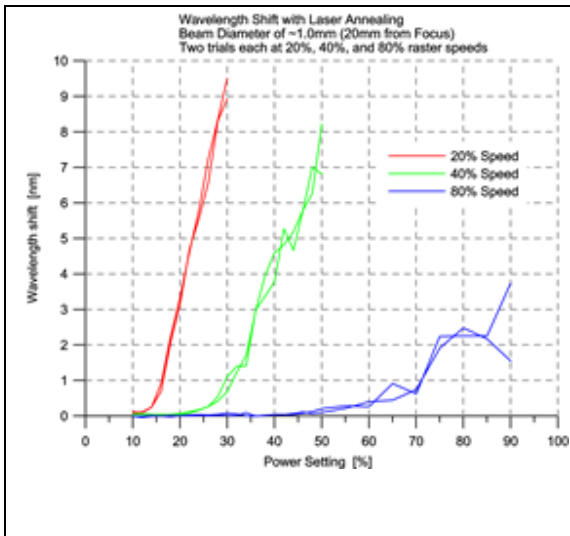


Figure 13: Wavelength shift (nm) is plotted as a function of power setting (%) for three raster speeds. Both power and dwell time are viable controls in locally controlling wavelength adjustment.

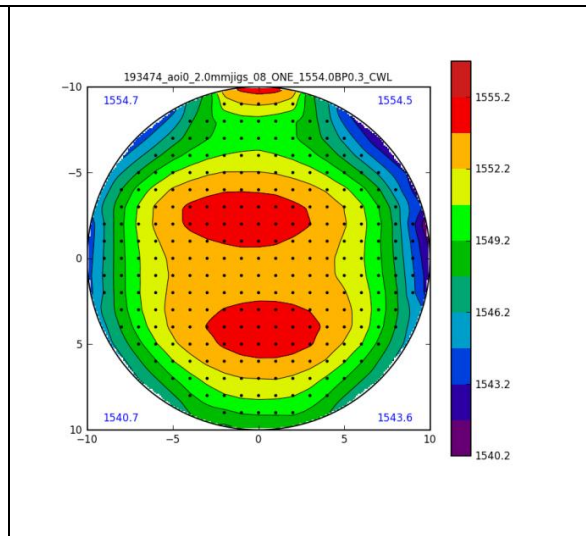


Figure 14: Center wavelength of an ultra-narrow band pass filter is plotted as a function of location on a 200 mm plate prior to laser targeted annealing.

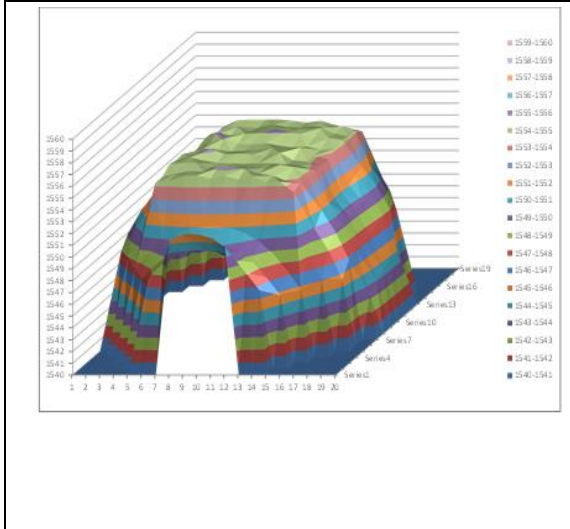


Figure 15: Laser Targeted Annealed single cavity bandpass filter: Ave=1554.61 nm/Stdev = 0.279 nm. The target wavelength was 1554.6

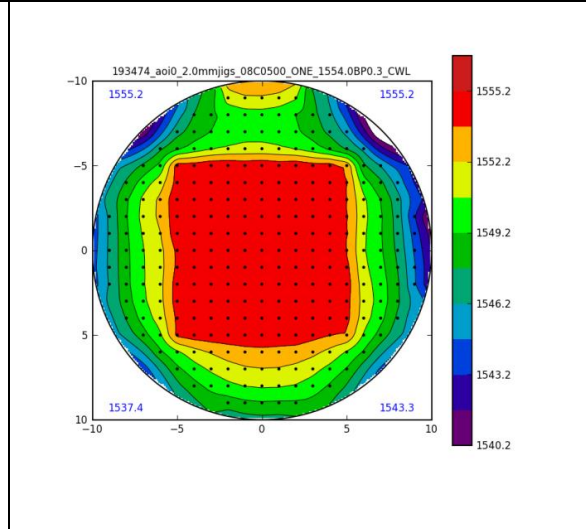


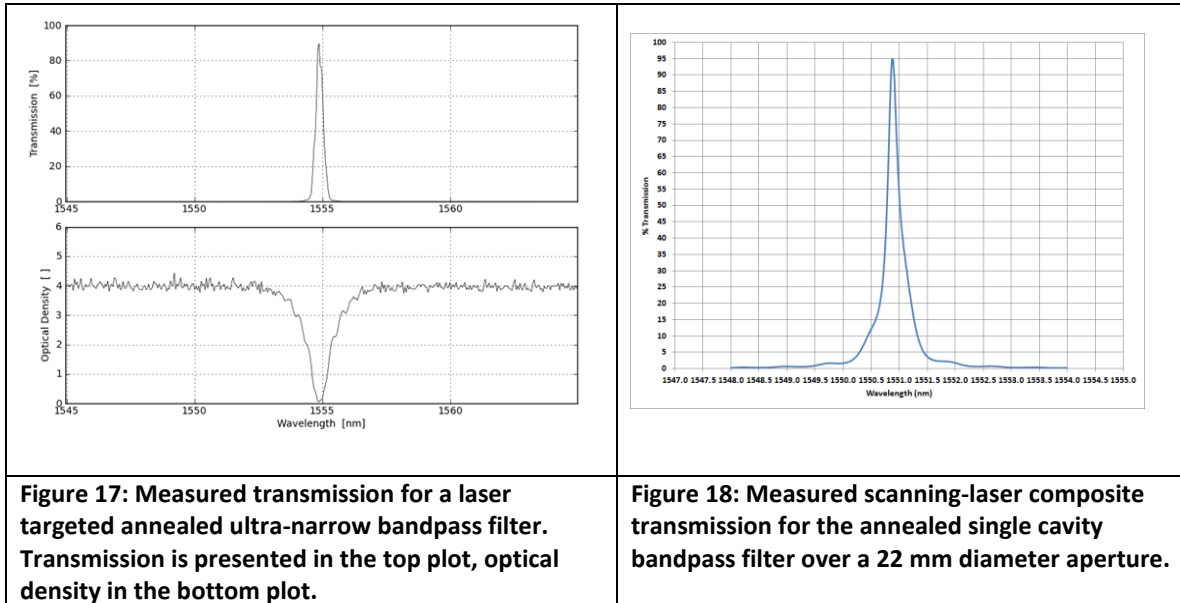
Figure 16: The center 110 x 110 mm region was laser targeted annealed. The data shows that the center area has been annealed uniform to +/- 0.05%.

Figures 17 and 18 present measured transmission scans of two filters fabricated using post process annealing and demonstrating good control of the center wavelength and composite performance over a 25 mm sample.

Conclusions

Post process annealing is an effective means of controlling a filter's center wavelength and meeting the high level of performance uniformity needed for ultra-narrow band pass filters. These filters are hard oxide coatings with a high degree of performance and environmental

stability. With proper selection of substrate ^{7,8}, the thermal sensitivity of these films can be tuned to better than 0.02 nm per degree C. Compensation for laser drift or Doppler shift can be accommodated using a heater.



Acknowledgement: This work was support by NASA/JPL contract NNX17CP58P.

References:

1. Deep Space Communications via Faraway Photons, October 18, 2017, <https://www.jpl.nasa.gov/news/news.php?feature=6967>
2. Deep Space Optical Communications (DSOC) https://www.nasa.gov/mission_pages/tmd/dsoc/index.html
3. [Macleod](#), H. Angus; [Thin-Film Optical Filters (Optics and Optoelectronics Series) / Edition 4, 2010], Taylor and Francis. ISBN-10: 1420073028
4. Rahmlow, Thomas D., Fredell, Markus, Chanda, Sheetal, Johnson, Robert L., "Ultra-narrow bandpass filters for infrared applications with improved angle of incidence performance", Proceedings of SPIE Vol. 9822, 982211 (2016)
5. [Fredell](#), Markus A.; [Carver](#), Gary E. ; [Chanda](#), Sheetal ; [Locknar](#), Sarah A. [and Johnson](#), Robert L.; " Sub-nanometer band pass coatings for LIDAR and astronomy ", Proc. SPIE9612, Lidar Remote Sensing for Environmental Monitoring XV, 96120K (September 1, 2015)
6. Ziter, Mark; Carver, Gary; Locknar, Sarah, Johnson, Jr., Robert; Laser-based assessment of optical interference filters with sharp spectral edges and high optical density; [Surface and Coatings Technology](#) 241:54–58 · January 2014
7. Brown, Jeffrey; "Center wavelength shift dependence on substrate coefficient of thermal expansion for optical interference filters deposited by ion beam sputtering", Applied Optics, Vol 43, No 23, 10 Aug 2004.
8. Sung-Hwa Kim and Chang Kwon Hwangbo, "Derivation of the center wavelength shift of narrow-bandpass filters under temperature change", Optics Express 5634, 15 Nov 2004.